Chapter III

PREPARATION AND CHARACTERISATION OF Sb$_2$S$_3$ THIN FILMS FROM AQUEOUS MEDIUM

3.1 INTRODUCTION

Recently considerable attention has been given to the preparation of thin metal chalcogenide films for a solar cell applications by various techniques [1-6]. Many binary and ternary semiconductors on a variety of substrates have been prepared by the spray pyrolysis techniques [7-9]; the more important examples being CdS, CdSe, CdTe, $CuInS_2$, $CuInSe_2$, Bi_2CdS_4, $CdSb_2S_4$, $Cd_xSe_xS_{1-x}$, $Cd_xZn_{1-x}S$, FeS_2 etc. However, few reports are available in the literature on the preparation of Sb_2S_3 thin films by spray pyrolysis.

In spray pyrolysis method, the materials required to form the desired semiconductor are taken in the solution form and then sprayed onto preheated substrates maintained at desired temperature, resulting in the formation of thin films on the substrates. When spray starts, pyrolytic decomposition of the solution occurs and uniform, well adherent films are resulted. The other volatile byproducts and excess solvent escape in the form of vapour. The thermal energy for decomposition and subsequent recombination of the species and the sintering and recrystallisation of the crystallites is provided by the hot substrate. It is different for the different materials and for the different solvents used in the spray process.

In this chapter, experimental arrangement of spray pyrolysis technique is described in detail. The optimized preparative parameters for deposition of Sb_2S_3 thin films from aqueous medium are reported. The structural, optical and electrical properties of these films are studied and discussed.

3.2 EXPERIMENTAL

3.2.1 Thin film deposition

3.2.1.1 Spray pyrolysis technique

The Schematic diagram of the spray pyrolysis technique is shown in Fig. 3.1. It mainly consists of spray nozzle, rotor for spray nozzle, liquid level monitor, hot plate, gas regulator valve and air tight fibre chamber.

a) Spray nozzle

It is made up of corning glass and consists of the solution tube surrounded by the glass bulb. With the application of pressure to the carrier gas, the vaccum is created at the tip of the nozzle and the solution is automatically sucked in the solution tube and the spray starts.

b) Rotor for spray nozzle

Stepper motor based microprocessor controller is used to control the linear simple harmonic motion of the spray nozzle over the required length of the substrates.

c) Liquid level monitor

The spray rate at a fixed air pressure depends upon the height of the solution measured with respect to the tip of the nozzle. The arrangement for the change in height of the solution forms the liquid level monitor.

d) Hot plate

Round, cast iron plate to which 2000 Watt heating coil fixed is used as a hot plate. Maximum temperature of 600 ^{o}C can be obtained with this arrangement. The chromel- alumel (26 guage) thermocouple is used to measure

Fig. 3.1 Schematic set-up for spray pyrolysis technique
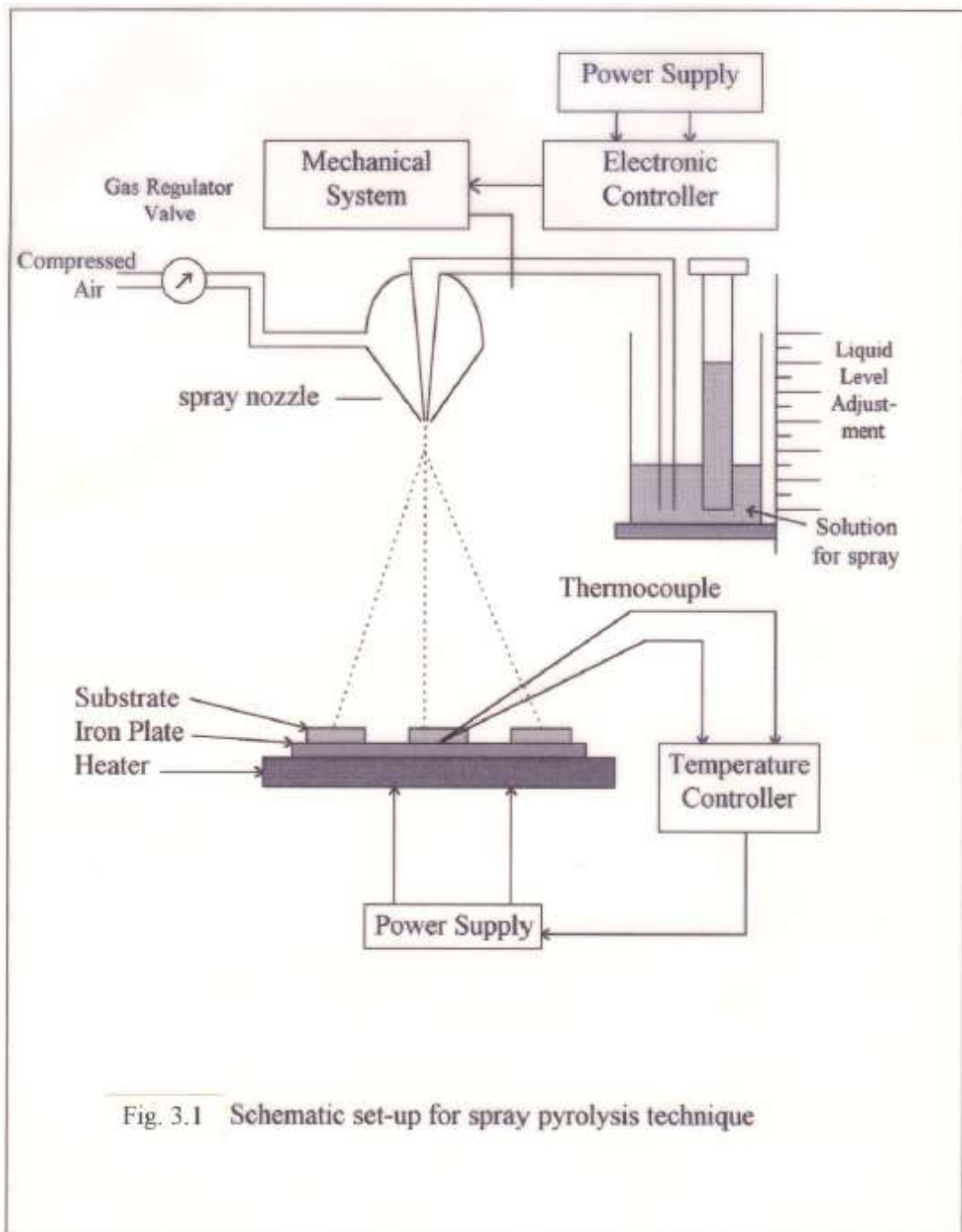
the temperature of the substrates and is fixed at the center of the front side of the iron plate. The temperature of the hot plate is monitored with the help of temperature controller [Aplab make Model No. 9601].

e) Gas regulator valve

The gas regulator valve is used to control the pressure of the carrier gas flowing through the gas tube of the spray nozzle. A corning glass tube of length 25 cm and of diameter 1.5 cm is converted into gas flow meter. Since air pressure depends upon the size of the air flow meter, the air flow meter should be calibrated from nozzle to nozzle.

f) Air tight fibre chamber

Since the number of toxic gases are evolved during the thermal decomposition of sprayed solution, it is necessary to fix the spraying system inside an air tight fibre chamber. An air tight fibre chamber of the size (2 " X 2 " X 2 ") was fabricated. To avoid the corrosion of the chamber, it is made up of fibre. The outlet of chamber is fitted to exhaust fan to remove the gases envolved during thermal decomposition.

3.2.1.2 Substrate cleaning

In thin film deposition process substrate cleaning is an important factor to get reproducible films as it affects the smoothness, uniformity, adherence and porosity of the films. The substrate cleaning process depends upon the nature of the substrate. The common contaminates are grease, adsorbed water, air borne dust, lint, oil particles, etc. The microslides supplied by Blue Star of

dimensions 7.8cm x 2.2cm x 0.1cm have been used as the substrates. The following process has been adopted for cleaning the substrates.

1) The substrates were washed with detergent solution 'Labolene' and then with water.

2) These substrates were boiled in chromic acid for about five minutes.

3) Substrates were cleaned with distilled water.

4) These substrates were kept in NaOH solution to remove the acidic contaminations.

5) The substrates were again washed with distilled water and cleaned ultrasonically.

6) Finally substrates were dried in alcohol vapours.

3.2.1.3 Preparation of solutions

Initial ingradients used to deposit Sb_2S_3 thin films from aqueous medium are as follows :

i) A.R. Grade antimony trichloride [$SbCl_3$] supplied by s.d. fine chem. Limited, Boisar, Mumbai.

ii) A.R. Grade tartaric acid [$C_4H_6O_6$] supplied by s.d. fine chem. Limited, Boisar, Mumbai.

iii) A.R. Grade hydrochloric acid [HCl] supplied by s.d. fine chem. Limited, Boisar, Mumbai and

iv) A.R. Grade thioacetamide [CH_3CSNH_2] supplied by Loba chem., Mumbai.

Solution of $SbCl_3$ was prepared by dissolving appropriate amount of it into concentrated hydrochloric acid and was then diluted using deionised

double distilled water to get the required volume. Tartaric acid and thioacetamide were dissolved in deionised double distilled water.

3.2.1.4 Deposition of Sb$_2$S$_3$ thin films

Thin films of Sb$_2$S$_3$ were deposited by spraying tartaric acid complex of SbCl$_3$ and CH$_3$CSNH$_2$ onto preheated amorphous glass substrates by taking their equimolar solutions in appropriate volumes so as to obtain Sb:S ratio of 2:3. The spray rate was kept constant at 5 cc min^{-1}. 3 cc solution of tartaric acid was mixed with 6 cc of SbCl$_3$. Then 9 cc of CH$_3$CSNH$_2$ solution was added into complexed SbCl$_3$ and immediately sprayed onto the hot glass substrates maintained at desired substrate temperature. The films are allowed to cool to a room temperature and are taken out of the deposition chamber to preserve them in dark dessicator.

3.2.1.5 Annealing of the Sb$_2$S$_3$ thin films

The Sb$_2$S$_3$ thin films were annealed in nitrogen atmosphere at temperature of 300^{0}C for 2 hours in high temperature tabular furnace supplied by Taurs and Associates, Adyar, Madras.

3.2.2 CHARACTERISATION OF Sb$_2$S$_3$ THIN FILMS

The structural, optical and electrical characterisation of the films deposited at optimised preparative parameters was carried out by means of X-ray diffraction, Scanning Electron Microscopy (SEM), optical absorption, dark electrical resistivity and TEP measurement techniques.

3.2.2.1 X-Ray diffraction (XRD)

The structural characterisation of Sb_2S_3 thin films was carried out by analyzing the X-ray diffraction patterns obtained using a Philips X-ray diffractometer model PW- 1710 (λ = 1.5405 Å for Cu-Kα radiation).

3.2.2.2 Scanning Electron Microscopy (SEM)

Microstructural aspects of the films were studied with SEM microscopes. The films were coated with gold-palladium (Au-Pd) of thickness 150 Å using Polaron SEM sputter coating with, E-2500. The SEM micrographs are obtained with Cambridge Stereoscan 250- MK3 assembly.

3.2.2.3 Optical absorption

Optical absorption studies were carried out using a UV-Vis-NIR Spectrophotometer (Hitachi model - 330, Japan) in the wavelength range of 350-850 nm.

3.2.2.4 Electrical resistivity

The two point d.c. probe method was used to study the variation of restivity with temperature. The experimental setup is schematically shown in Fig. 3.2. The brass plate of size 10 cm x 5 cm x 0.5 cm is grooved at the bottom side so as to fit the heating elements (Toni 60 Watt) parallel to the length of the plate, in order to achieve the uniform temperature. The sample is mounted on the top of the plate. The thin film of size 1 cm x 1 cm x 0.5 μm on glass substrate is used for the resistivity measurement. Silver paste was applied for making the good ohmic contacts to the film [10-11]. A mica sheet
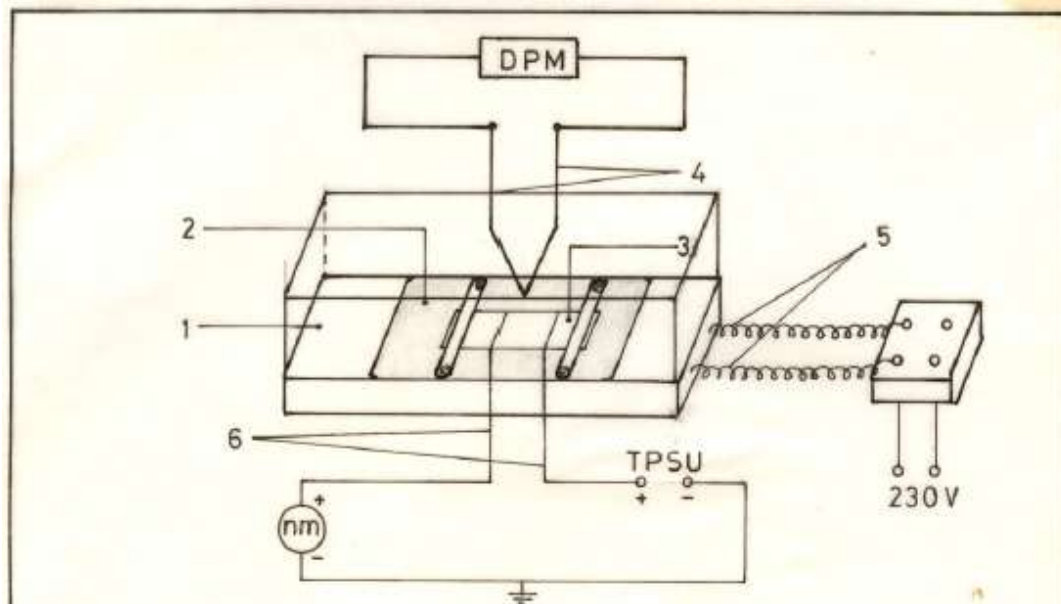
1 – Specimen holder (Brass) ; 2 – Mica sheet ;
3 – Sample (thin film) ; 4 – Thermocouple ; 5 – Heater ;
6 – Copper wire .

Fig. 3.2

Schematic circuit diagram for the measurment of electrical
resistivity of thin film .
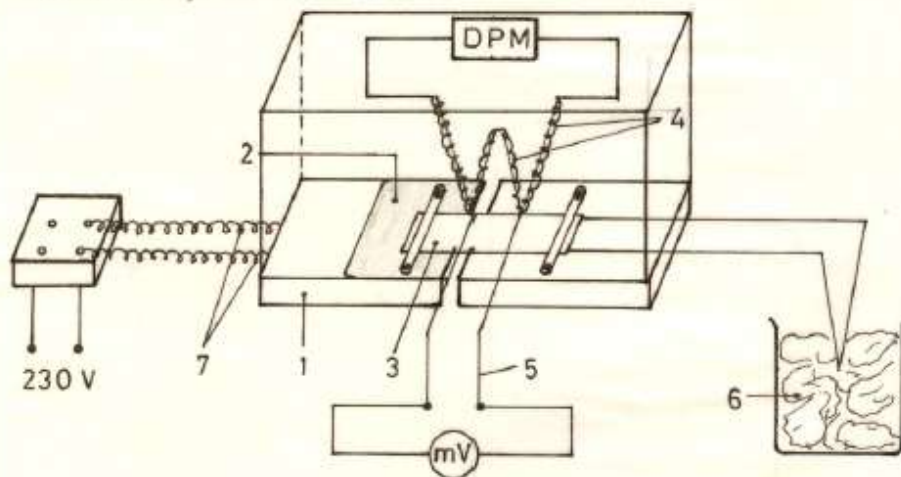
1 – Specimen holder (Brass) ; 2 – Mica sheet ;
3 – Specimen (thin film) ; 4 – Chromel Alumel
thermocouple ; 5 – Copper wire ; 6 – Ice ; 7 – Heater .

Fig. 3.3

Schematic circuit diagram of the TEP measurment .

was used between the film and the brass plate to provide the insulation. The temperature is measured with chromel-alumel thermocouple which is fixed at the center of the sample. The temperature was recorded on digital panel meter (0 to 199.9 mV range) (DPM) supplied by Omega Electronics, Jaipur. Aplab power supply is used for passing current through the film and the current was measured with TestroniX-8 digital d.c. micro ammeter.

3.2.2.5 *Thermoelectric power (TEP)*

A schematic diagram for the thermoelectric power measurement set up is shown in Fig. 3.3. A brass block gives the uniform temperature gradient along the length of the sample holder. The sample holder was fixed on porcelain base. The films of size (1x1) cm^2 on glass substrates were used for TEP measurement. Silver paste was used for insuring perfect contacts [11]. A mini heater was used for heating one end of the sample; another end being in an ice. A differential chromel-alumel thermocouple was used to measure the temperature gradient across the sample and a separate chromel-alumel thermocouple was used to measure the mean temperature. The thermocouple voltage was measured with DPM supplied by Omega Electronics, Jaipur. The thermoelectric voltage was measured by TestroniX-8 digital d.c. micro volt-ammeter. The circuit diagram for the measurement of TEP is shown in Fig. 3.4.
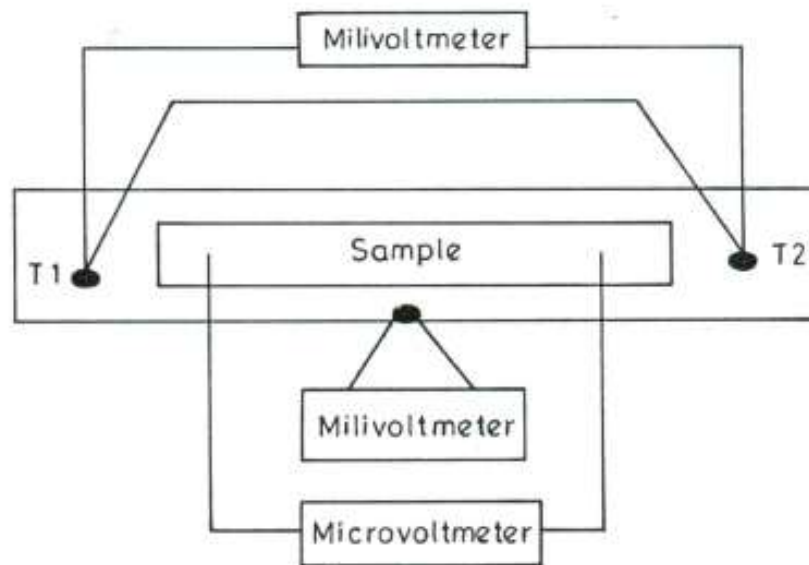
Fig. 3·4 – Circuit diagram for measurement of
thermoelectric power (TEP).

3.3 RESULTS AND DISCUSSION

The direct mixing of SbCl$_3$ and CH$_3$CSNH$_2$ solution results in a yellowish turbidity which prohibits the spraying process. Tartaric acid forms a strong complex with antimony, and therefore the addition of thioacetamide solution does not cause this sort of turbidity. This mixed solution remains stable for about 10 min. The various preparative parameters viz. spray rate, substrate temperature, solution concentration, concentration of complexing agent etc. were optimised as discussed in the next section.

3.3.1 Optimization of preparative parameters

3.3.1.1 Spray rate

The spray rate is one of the important preparative parameters in thin film deposition by the spray pyrolysis technique. It can be varied either by changing the air pressure of the carrier gas or the height of liquid level monitor. During the Sb$_2$S$_3$ film deposition from aqueous medium the spray rate was maintained to be 5 cc min^{-1}.

3.3.1.2 Substrate temperature

To optimise the substrate temperature, the solution having concentration of 0.1 M is sprayed with spray rate 5 cc min^{-1} onto the set of glass substrates (microslides) which are maintained at temperatures 260, 280, 300, 320 and 340°C. The films deposited at substrate temperatures less than 280 ^{o}C are not adherent. This may be attributed to incomplete thermal decomposition of the sprayed solution. The dark-gray coloured films are formed at temperatures 280, 300 and 320°C. Above 320 ^{o}C, the films are not formed due to complete

thermal decomposition of the solution before reaching the glass substrates. After structural and electrical analysis, it has been found that the films prepared at 300 ^{o}C have relatively higher conductivity than the films deposited at 280 and 320 ^{o}C. Thus 300 ^{o}C is fixed as the optimised temperature for film deposition [7,12]

3.3.1.3 concentration of complexing agent

In the present work, tartaric acid was used as a complexing agent, for the deposition of the films from aqueous medium. To optimize the concentration of tartaric acid, films were deposited using various concentrations of tartaric acid between 0.25 to 1 M in steps of 0.25 M and keeping optimised substrate temperature of 300 ^{o}C, spray rate of 5 cc min^{-1} and concentration of solution of 0.1M. It has been found that for the concentration less than 0.25M of tartaric acid sulphide precipitate formation occurs before spraying process starts. Sb_2S_3 compound formation does not take place for concentration (> 1M) of tartaric acid, due to strong complex formation of Sb^{3+}. On the other hand, uniform black-gray coloured films result for the concentration of tartaric acid between 0.25 - 1.00 M. The structural and electrical characterisation studies show that the films prepared at concentration of 0.5M are uniform, and well adherent to the glass substrates and show relatively higher electrical conductivity compared to films with other concentrations. Therefore, 0.5M is resulted as the optimised concentration of complexing agent for Sb_2S_3 thin film preparation [12].

3.3.1.4 Concentration of spraying solution

To optimise the concentration of solution substrate temperature and concentration of complexing agent were kept constant at their optimized values as 300 $^{\circ}$C and 0.5 M respectively. The films were prepared at solution concentrations 0.025, 0.050, 0.075, 0.1 and 0.150 M respectively. The spray rate was maintained to be 5 cc min^{-1}. It is seen that the films prepared at concentration 0.15 M are porous, non-uniform and not adherent to the substrate. The film formation does not observed below concentration of 0.025 M. This may be due to unsuitable substrates temperature. At higher concentrations the complete thermal decomposition of solution does not take place and the concentration of the tartaric acid is not sufficient to form a strong complex. The black-gray films are formed corresponding to concentrations between 0.025 - 0.15 M. Electrical studies show that the films prepared at concentration of 0.075M show relatively higher electrical conductivity. Therefore, 0.07M concentration of spraying solution is taken as the optimized concentration for the film preparation [13].

3.3.2 Thickness measurement

The thickness of the prepared thin films was determined using relation 2.1 by a gravimetric method. The density of the deposited material is assumed to be the same as that of the bulk material (ρ= 4.1 gm cm^{-3} for Sb_2S_3).

The thickness of Sb_2S_3 films is found to be of the order of 0.5μm and depends on concentration of spraying solution and the concentration of complexing agent [12 - 13].

3.3.3 X-ray diffraction

The structural properties of the film were studied from XRD patterns and are shown in Fig. 3.5. The appearance of the broad X-ray spectrum suggests that the films are either amorphous or of poor crystallinity.The as prepared Sb_2S_3 films are observed to be amorphous by many workers [14 - 20].

3.3.4 Scanning Electron Microscopy (SEM)

SEM micrographs of Sb_2S_3 thin films deposited onto glass substrates are studied to see the surface morphology of the film. SEM micrographs of Sb_2S_3 film are shown on Fig. 3.6 (a to c) for three different magnifications. The film clearly demonstrates an uneven surface morphology with irregular particle growth. The total coverage of the substrate surface by the film with random distribution of overgrown particles is also seen.

3.3.5 Optical absorption

The Sb_2S_3 thin films are characterized by measuring the optical density (αt) in the wavelength range 350 to 850 nm. The variation of the absorption coefficient α with wavelength λ for the Sb_2S_3 film is shown in Fig. 3.7. The film shows cut-off at 6900Å. The bandgap (Eg) is estimated by extrapolating
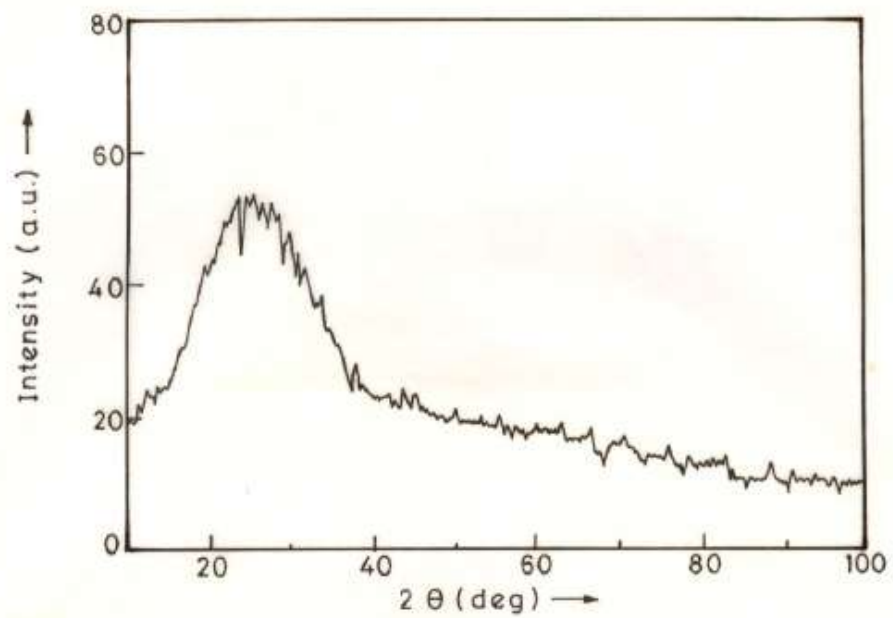
Fig. 3·5 – XRD pattern of Sb_2S_3 thin films from aqueous medium.

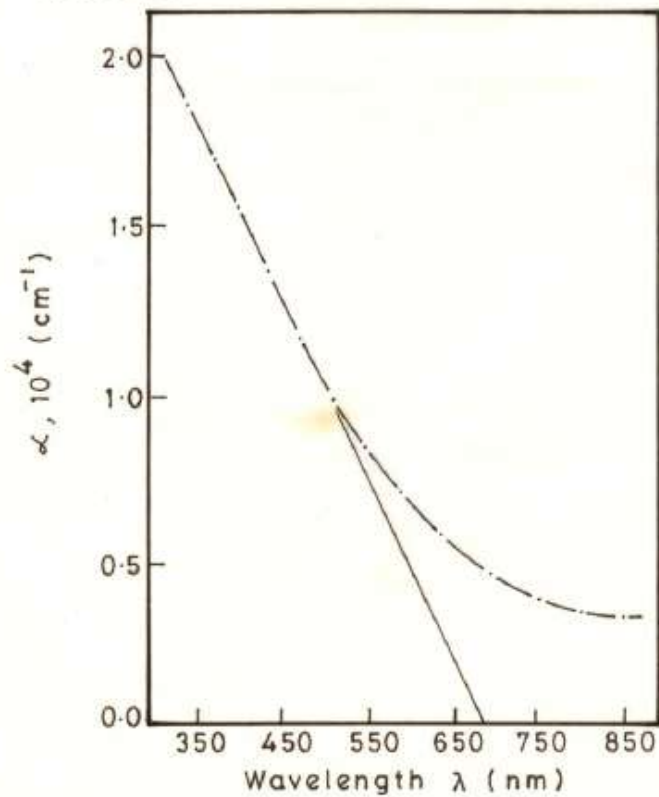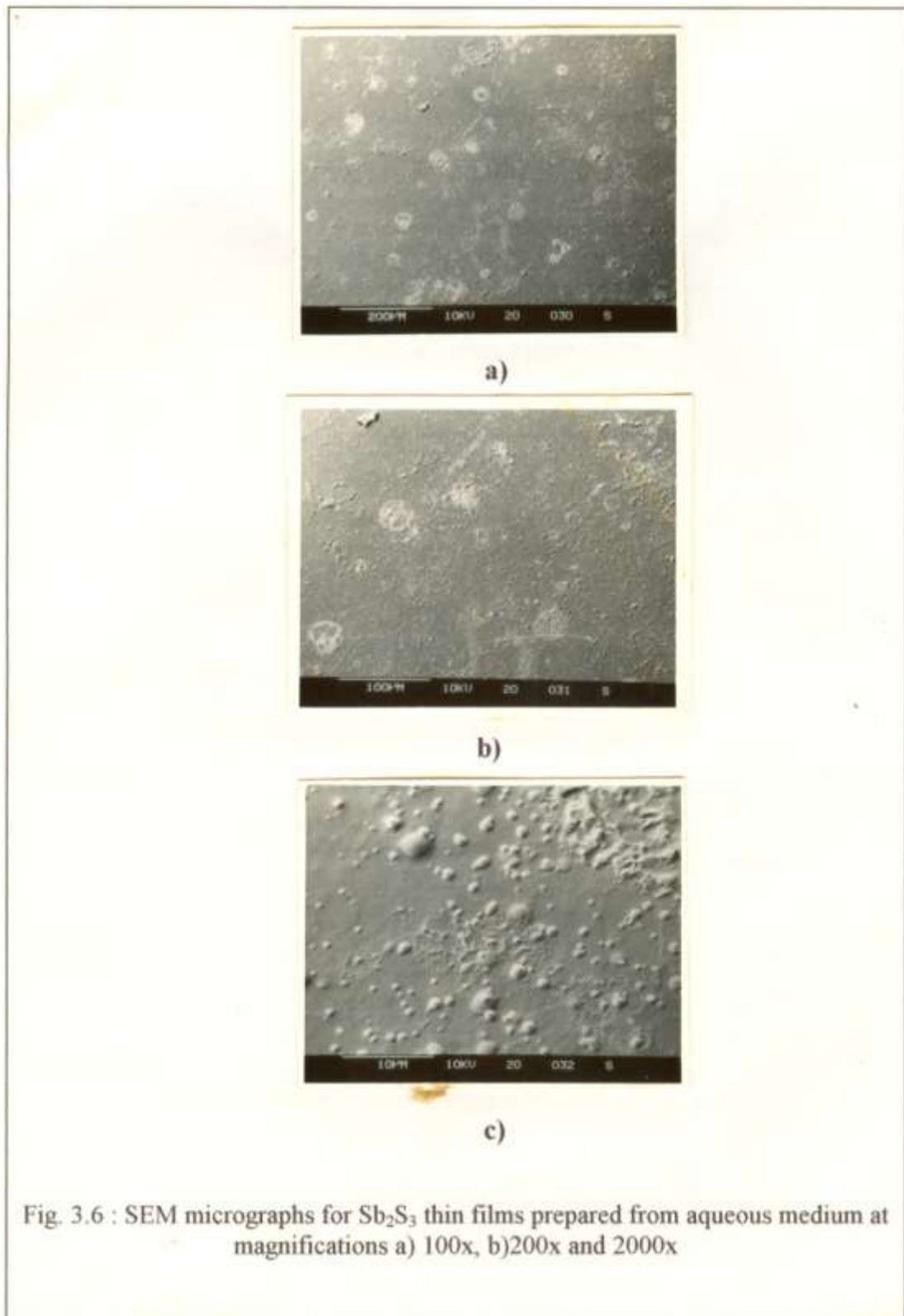Fig. 3·7 – Plot of absorption coefficient vs wavelength for Sb_2S_3 thin film.

a)

b)

c)

Fig. 3.6 : SEM micrographs for Sb_2S_3 thin films prepared from aqueous medium at magnifications a) 100x, b)200x and 2000x

the straight line portion to wavelength axis as reported by many workers [21-25]. The optical gap is found to be 1.8 eV, which is in good agreement with the value of the optical gap reported earlier [18,21,26] for Sb_2S_3.

3.3.6 Electrical Resistivity

Two point d.c. dark resistivity measurement shows that the Sb_2S_3 films are highly resistive. The dark resistivity is of the order of 10^6 - $10^7 \Omega$.cm similar to the results of others [7,18-19, 26-28]. The variation of log (ρ) with reciprocal of temperature is depicted in Fig. 3.8. It is seen that the resistivity decreases with increase in temperature and supports the semiconducting nature of the Sb_2S_3 films. The estimated activation energy is equal to 0.52 eV, agreeing with that reported earlier [21]. The electrical activation energy, $\Delta E < (1/2)$ Eg, for the most amorphous semiconductors, so the Fermi level lies near the center of the gap [29]. The presence of certain structural defects (in microcrystalline Sb_2S_3 thin films) and their resulting states in the gap give 'tailing' of states into the gap for this reason. The relationship between the activation energy and the band gap is not true in this case.

3.3.7 Thermoelectric Power (TEP)

The thermoelectric power measurements were used to knoe the type of conductivity of the material. The dependence of TEP on temperature is depicted in Fig. 3.9, it is seen that the polarity of thermoelectric voltage for Sb_2S_3 film is positive towards the hot end, indicating the Sb_2S_3 is n-type in nature. The plot shows that the increase in temperature results increase in
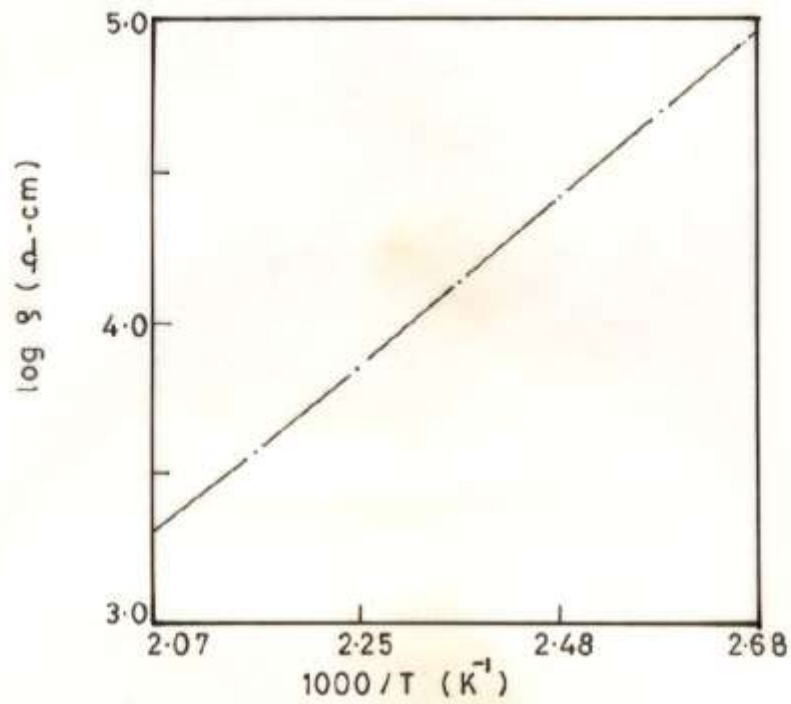
Fig. 3·8 — Plot of log ς against 1000/T for Sb$_2$S$_3$ thin film.
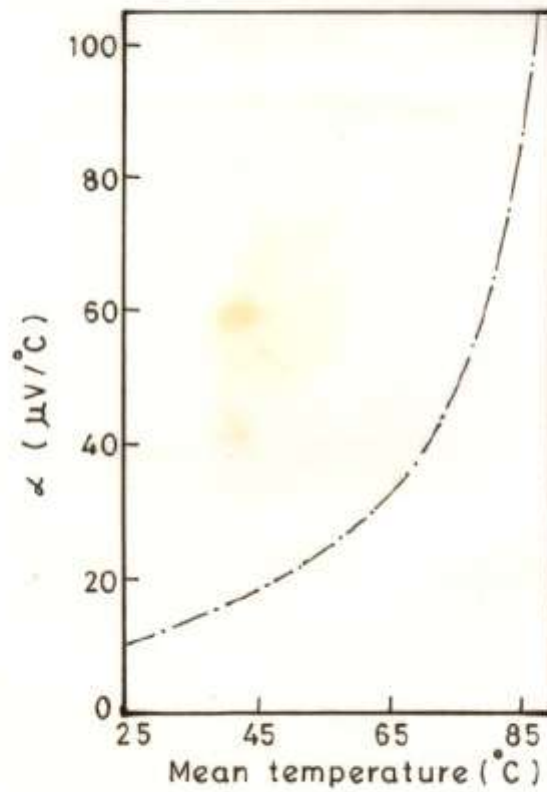

Fig. 3·9 — Variation of seeback coefficient against the mean temperature for Sb$_2$S$_3$ thin film.

Seebeck coefficient may be due to the increase in carrier concentration and mobility of charge carriers with rise in temperature.

The Sb_2S_3 thin films were annealed in nitrogen atmosphere at temperature of 300^0C for 2 hours in order to see the effect of annealing on structural and electrical properties. It is seen that there is no any change in structure and order of room temperature resistivity of the films after annealing. This may be due to non- stoichiometric proportion of Sb and S in Sb_2S_3 thin films.

REFERENCES

1. K.L. Hardee and A.J. Brad, J. Electrochem. Soc., 122 (1975) 739.

2. N.R. Pawaskar, C.A. Menezes and A.P.B. Sinha, J. Electrochem. Soc., 124 (1977) 743.

3. R.R. Chamberlin and J.S. Skarman, J. Electrochem. Soc., 113 (1966) 86.

4. S.P. Wolsky, Trans. 10th Natl. Vaccum Symp., The Macmillan Company, New York, (1963)

5. H.M. Francombe, Trans. 10th Natl. Vacuum Symp., The Macmillan Company, New York, (1963).

6. S. Dushman, Scientific Foundation of Vacuum Technique, 2nd Ed., Ed. J.M. Lafferty, John Wiley and Sons., Inc., New York, (1962).

7. C.H. Bhosale, M.D. Uplane, P.S. Patil and C.D. Lokhande, Thin Solid Films, 248 (1994) 137.

8. H.S. Soni, S.D. Sataye and A.P.B. Sinha, Ind. J. Pure and Appl. Phys., 21 (1982) 197.

9. S.K. Pawar and S.H. Pawar, Mat. Res. Bull., 18 (1983) 211.

10. R.N. Bhattacharya and P. Pramanik, J. Electrochem. Soc., 129 (1982) 332..

11. J.P. Mitchell and D.G. Denure, Thin Solid Films, 16 (1973)285.

12. K.Y. Rajpure, C.D. Lokhande and C.H. Bhosale, Mater. Chem. Phys., 51 (1997) 252.

13. K.Y. Rajpure and C.H. Bhosale, in Physics of Semiconductor Devices (IWPSD - 97), Volume - II, Eds. V. Kumar and S.K. Agarwal, Narosa Publishing House, New Delhi, (1998), p. 1233.

14. K.C. Mandal and A. Mondal, J. Phys. Chem. Solids, 51 (1990) 1339.

15. O. Savadogo and K.C. Mandal, Sol. Ener. Mater. Solar Cells, 26 (1992) 117.

16. I. Grozdanov, Semicond. Sci. Technol., 9 (1994) 1234.

17. M.T.S. Nair, Y.Pena, J.Campos, V.M. Garcia, and P.K. Nair, J. Electrochem. Soc., 145 (1998) 2113.

18. J.D. Desai and C.D. Lokhande, Bull. Electrochem., 9 (1993) 242.

19. J.D. Desai and C.D. Lokhande, Thin Solid Films, 237 (1994) 29.

20. C. Ghosh and B.P. Verma, Solid State Commun., 31 (1979) 683.

21. C.D. Lokhande, Ind. J. Pure and Appl. Phys., 29 (1991) 300.

22. S.H. Pawar, S.P. Tamhankar, P.N. Bhosale and M.D.Uplane, Ind. J. Pure and Appl. Phys., 21 (1983) 665.

23. M.D. Uplane and S.H. Pawar, Solar Cells, 10 (1983) 177.

24. S.F. McCann and M.S. Kazacos, J. Electroanal. Chem., 119 (1981) 109.

25. E.A. Davis and E.L. Lind, J. Phys. Chem. Solids, 29 (1968) 79.

26. V.V. Killedar, C.D. Lokhande and C.H. Bhosale, Mat. Chem. Phys., 47 (1997)104.

27. C.D. Lokhande, Mat. Chem. Phys., 28 (1991) 145.

28. J.D. Desai and C.D. Lokhande, J. Non-Cryst. Solids, 181 (1995) 70.

29. S.R. Elliott, Physics of Amorphous Materials (Longman, London, 1983) p.212.